Analytical Methods

Accepted Manuscript

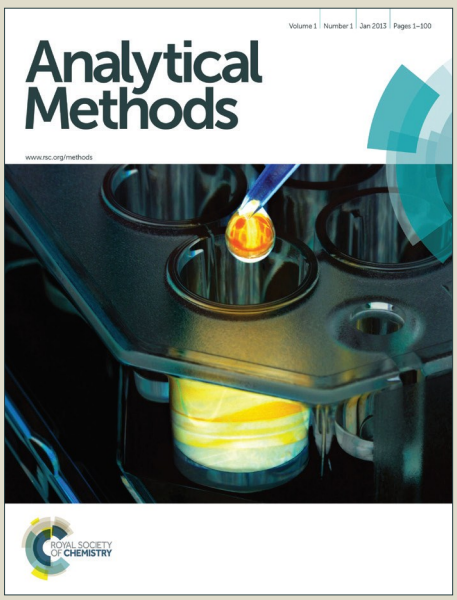

This is an *Accepted Manuscript*, which has been through the Royal Society of Chemistry peer review process and has been accepted for publication.

Accepted Manuscripts are published online shortly after acceptance, before technical editing, formatting and proof reading. Using this free service, authors can make their results available to the community, in citable form, before we publish the edited article. We will replace this *Accepted Manuscript* with the edited and formatted *Advance Article* as soon as it is available.

You can find more information about *Accepted Manuscripts* in the Information for Authors.

Please note that technical editing may introduce minor changes to the text and/or graphics, which may alter content. The journal's standard Terms & Conditions and the Ethical guidelines still apply. In no event shall the Royal Society of Chemistry be held responsible for any errors or omissions in this *Accepted Manuscript* or any consequences arising from the use of any information it contains.

ROYAL SOCIETY OF CHEMISTRY

www.rsc.org/methods

Analytical Methods

ARTICLE

A fluorophore-conjugated ascorbic acid functions for visualization of sodium vitamin C transporters in living cells

Received 00th January 20xx,
Accepted 00th January 20xx

DOI: 10.1039/x0xx00000x

www.rsc.org/

Junfa Yin, [a] Yuanyuan Song, [a] Ning Zhang, [a,b] Tian Xu [a] and Hailin Wang [a,*]

Human beings do not produce ascorbic acid (AA) and acquire AA through the sodium vitamin C transporters (SVCTs). Changes in expression or function of SVCTs proteins may be associated with human diseases. In this regard, imaging of SVCTs in living cells is meaningful. However, the options for live-cell labeling of SVCTs were very limited. In this work, we synthesized a new small-molecule fluorescent probe RB-A-Vc, and demonstrated its application in selectively visualizing SVCTs in living cells. This probe features visible excitation and emission profiles, ease of entering into membrane, high selectivity for SVCTs, and can monitor up-regulation or down-regulation of SVCTs expression in living cells. We emphasize this small-molecule probe is suitable for subcellular localization of SVCTs in living cells. This study provides a useful tool for simultaneously monitoring the level and distribution of intracellular SVCTs, which is probably more meaningful to evaluate the changes induced by exoteric stimulations. We propose that this probe for SVCTs imaging and the corresponding method could be applied to other cell lines, tissues, and species.

Introduction

Ascorbic acid (AA, or vitamin C) is an essential nutrient for mammals.[1-3] It plays a key role in antioxidant defense against harmful free radicals.[4-6] Essentially, human beings do not synthesize vitamin C by themselves, and rely on the uptake of AA through the sodium vitamin C transporters (SVCTs), including SVCT1 and SVCT2.[7-9] SVCT1 is involed in whole-body homeostasis of AA, whereas SVCT2 protects metabolically active cells against oxidative stress. SVCTs are thus crucial for maintaining intracellular ascorbate levels.

Deficiency of SVCTs brings haemorrhage in lower brainstem areas and increased oxidative stress in several organs of mice,[10] even causes mice to die after birth, with respiratory failure and cortical brain haemorrhage.[11] Changes in expression or function of the SVCTs may be associated with human diseases including Huntington's disease, breast and prostate cancers, and colorectal adenoma.[12-15] Therefore, intracellular SVCT monitoring and detection can provide valuable information for biological diagnosis, adaptive therapy and drug discovery.[16-18] In this regard, live-cell imaging of SVCTs is meaningful because it can provide high spatiotemporal resolution for the analysis of SVCTs dynamics, reflects the ascorbate transporters expression levels, subcellular distribution and spatiotemporal dynamics. Up to now, the options for live cell labelling of SVCTs were very limited. The antibodies against SVCT1 and/or SVCT2 in immunofluorescence assays are not membrane permeable. Thus they can only be used for indicating SVCTs in fixed and permeabilized cells.[19,20] Another important issue is, although antibodies for SVCT1 and SVCT2 are provided, there is lack of a reporter for monitoring the globe level and changes of SVCTs. In fact, the previous studies revealed that the biological and toxicological functions of AA transporters are commonly associated with both SVCT1 and SVCT2.[1, 2, 9] To the best of our knowledge, up to date, there are no fluorescent probes capable of selective detection of the total SVCTs in living cells. The development of easy-to-use probes, which can pass the cell membrane and selectively bind and illuminate the total SVCTs, was thus required.

Herein, we synthesized a fluorophore-conjugated vitamin C (RB-A-Vc), and demonstrated its application in selectively visualizing SVCTs in living cells. The unique merits of this study include, 1) the synthesized small-molecule compound can easily pass through cell membrane by binding to SVCTs and thus is suitable for living cells imaging, and 2) being a potent tool for simultaneously visualizing the level and changes of the total intracellular SVCTs.

Experimental

Reagents and materials

L-ascorbic acid (AA), phorbol 12-myristate 13-acetate (PMA), Triton X-100, Tween 20 and 4',6-diamidino-2-phenylindole (DAPI) were purchased from Sigma-Aldrich (MO, USA). Lissamine rhodamine B sulfonyl-chloride and 1,4-diethlene dioxide were from Acros (NJ, USA). 4-(Dimethylamino) pyridine (DMAP) and paraformaldehyde were from Alfa Aesar. 6-

[a] State Key Laboratory of Environmental Chemistry and Ecotoxicology, Research Center for Eco-Environmental Sciences, Chinese Academy of Sciences, Beijing 100085, People's Republic of China. E-mail: hlwang@rcees.ac.cn, Tel: +86-10-62849600.
[b] Shanghai Key Lab of Functional Materials Chemistry, East China University of Science and Technology, Shanghai 200237, China.

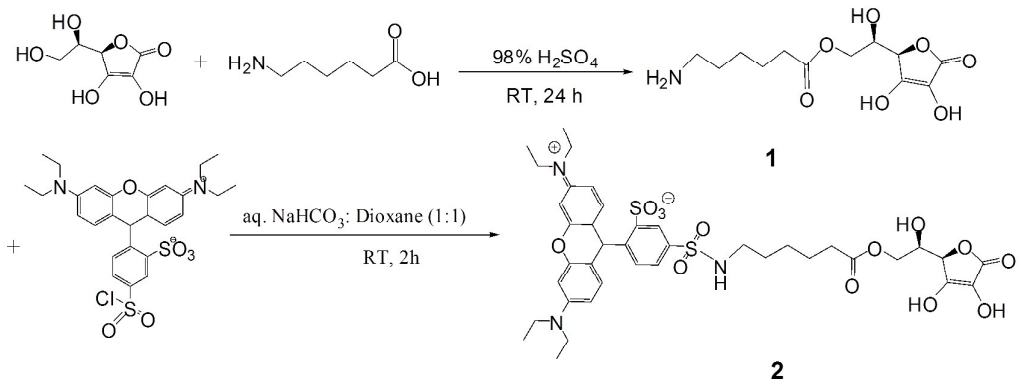

Scheme 1 Synthesis of sulforhodamine B-aminoheanoic acid-ascorbic acid ether (RB-A-Vc, **2**). RB-A-Vc was synthesized in two steps: 1) triggering the reaction of 6-aminoheanoic acid with L-ascorbic acid in sulfuric acid, producing aminoheanoic acid-ascorbic acid ester (A-Vc, **1**), and 2) conjugating sulforhodamine B onto A-Vc ester using 4-dimethylaminopyridine as the catalyst.

Aminoheanoic acid was from Sangon Biotech (Shanghai, China). $CaCl_2 \bullet 6H_2O$, NaCl, KCl, Na_2HPO_4, $NaHCO_3$ and KH_2PO_4 were purchased by Sinopharm Chemical Reagent Co, Lid (Beijing, China). Choline chloride was from J&K Co, Lid. (Beijing, China). Mito-Tracker Green and Dio were purchased by Beyotime Biotechnology (Shanghai, China).

Synthesis of sulforhodamine B-aminoheanoic acid-ascorbic acid ether (RB-A-Vc)

A mixture of 6-aminoheanoic acid (655 mg) and L-ascorbic acid (704 mg) were stirred in 98% H_2SO_4 (20 mL) for 24 h under nitrogen protection. The solution was diluted and neutralized to neutral and the residue was purified by solid phase extraction to give the product **1**. To a solution of **1** (29 mg) and DMAP (5 mg) in 1,4-diethlene dioxide-saturated aqueous sodium bicarbonate (500 µL: 500 µL), 40 mg of sulforhodamine B chloride was added and the reaction mixture was stirred at room temperature for 2 h. The residues were purified by silica gel column chromatography using trichloromethane/methanol (4:1, v/v) as the eluent to give the desired product **2** (RB-A-Vc). After rotary evaporation, the product was lyophilisated to solid and stored in -20 ^{0}C.

UHPLC-ESI-MS/MS analysis of RB-A-Vc

Sulforhodamine B-aminoheanoic acid-ascorbic acid ester (RB-A-Vc) was identified by reverse-phase UHPLC (Agilent 1290 UHPLC system) using a Zorbax Eclipse Plus C 18 column (2.1mm i.d. × 50 mm, 1.8 µm, Agilent Technologies, Palo Alto, CA) with a 6530 quadrupole tandem time of flight mass spectrometer (Agilent Technologies, Palo Alto, CA). The optimized mobile phase consists of 0.1% HCOOH (solvent A) and methanol (solvent B). The elution was 50% of B. The flow rate was set at 0.25 mL/min, the injection volume was 2 µL, and the column temperature was set at 25 ^{0}C. The mass spectrometer was operated in the positive ion mode. Nitrogen was used for nebulization and desolvation. The nebulization gas was set at 35 psi, the flow-rate of desolvation gas was 6 L/min, and source temperature was set at 200 ^{0}C. The sheath gas temperature was set at 300 ^{0}C and flow-rate was 10 L/min. Capillary voltage was set at 3500 V, and Nozzle Voltage 0 V. High purity nitrogen (99.999%) was used as the collision gas.

Cell culture

The human-derived hepatic epithelial HepG2 cells and the human cell line HEK-293T (supplied by cell culture centre, institute of Basic Medical Sciences, Chinese Academy of Medical Sciences, Beijing, China) were grown in RPMI 1640 medium and Dulbecco's modified Eagle's medium (DMEM)–high glucose (Hyclone, CE Healthcare Life Sciences) respectively supplemented by 10% foetal bovine serum (FBS, Gibco® Life technologies), 1% penicillin and streptomycin (Corning). The cells were cultured at 37 ^{0}C in a 5% CO_2 humidified atmosphere.

Confocal fluorescent imaging of SVCTs in fixed cells

HepG2 cells and HEK-293T cells were grown on 8-chamber glass-bottom dishes for 24 h, and then fixed in ice-cold 4% paraformaldehyde for 10 min and permeabilized with 0.1% Triton X-100 for 5 min. Then the cells were respectively cultured in RPMI 1640 and DMEM medium containing RB-A-Vc for 30 min. The cells were counterstained with DAPI to label nuclei, Mito-tracker green to label mitochondria, Dio to label plasma membrane for 10 min, and then analysed by confocal fluorescence microscopy.

Confocal fluorescent imaging of SVCTs in living cells

HEK-293T and HepG2 cells were seeded on 8-chamber glass-bottom dishes and incubated for one day. The cells were cultured in RPMI 1640 and DMEM medium containing RB-A-Vc (100 µM) for 30 min, respectively. The intracellular SVCTs can thus be visualized by confocal fluorescence microscopy directly.

For SVCTs localization investigations, the cells were needed to be fixed in 4% paraformaldehyde and permeabilized with 0.1% Triton X-100, counterstained with DAPI to label nuclei, mito-tracker green to label mitochondria and Dio to label plasma membrane.

To evaluate the dosage effect of RB-A-VC on SVCTs imaging, the cultured cells were respectively incubated in RPMI 1640 and DMEM medium containing RB-A-Vc (10 μM, 20 μM, 100 μM, 200 μM) for 30 min. Then the medium was removed, the cells were counterstained with DAPI, followed by the observation by confocal fluorescence microscopy.

Immunocolocalization of SVCTs in HEK-293T and HepG2 cells

For confocal fluorescence and colocalization experiments, HEK-293T and HepG2 cells were cultured in RPMI 1640 and DMEM medium containing RB-A-Vc (100μM) for 30 min, respectively. The stained cells were fixed in 4% paraformaldehyde for 10 min on ice, washed with BSS buffer (150 mM NaCl, 5 mM KCl, 1.9 mM KH_2PO_4, 1.1 mM Na_2HPO_4, 0.3 mM $MgSO_4 \bullet 7H_2O$, 1 mM $MgCl_2 \bullet 6H_2O$, 1.5 mM $CaCl_2 \bullet 2H_2O$, 10 mM HEPES, adjusted to pH 7.6 with NaOH), and permeabilized with 0.1% Triton X-100 (200 μL of 10% Triton-100 was diluted with 19.8 mL of BSS buffer) for 5 min. Afterwards, the cells were blocked with 5% non-fat dry milk in TBST (10 mL Tris-HCl pH 7.5, 8.8 g NaCl,1 mL Tween-20 in 1 L water) for 30 min, incubated for 3 h with primary antibodies: anti-SVCT1 (sc-9923 polyclonal, goat), anti-SVCT2 (sc-9926 goat polyclonal), anti-COXIV (ab-16056, rabbit polyclonal), anti-GLUT1 (ab-40084 mouse monoclonal), washed with BSS Buffer 3 times, and incubated for 1 h with fluorescent secondary antibodies: Fluorescein-conjugated affiniPure Donkey Anti-Mouse IgG(H+L) (ab10081) (in green fluorescence), Fluorescein-conjugated affiniPure Donkey Anti-Rabbit IgG (H+L) (ab10051) (in green fluorescence), Cy3-conjugated affiniPure Donkey Anti-Goat IgG (H+L) (ab10112) (in red fluorescence), Fluorescein-conjugated affiniPure Donkey Anti-Goat IgG(H+L) (00003-3) (in red fluorescence).

Cytoplasmic extraction and Western blot

Add protease inhibitors (1:100 dilution) and DL-Dithiothreitol (DTT) (1:1000 dilution) to CER I (Thermo Scientific) before use to maintain extract integrity and prevent oxidation. The adherent cells were harvested with trypsin-EDTA (Hyclone CE Healthcare Life Sciences) and centrifuged at 500 ×g for 5 minutes. After washing with BSS buffer, the cells was transferred to 1.5 mL microcentrifuge tube and centrifuged at 500 ×g for 3 minutes. The supernatant was carefully removed and discarded, leaving the cell pellet as dry as possible. After adding ice-cold CER I (100 μL) to the cell pellet, the tube was suspended for 15 seconds and incubated on ice for 10 minutes. Then the tube was added ice-cold CER II (5.5μL) and incubated for 1 minute. At last the tube was centrifuged for 5 minutes at maximum speed in a microcentrifuge (16,000 ×g) and the supernatant (cytoplasmic extract) was transferred to a clean pre-chilled tube. Protein concentrations were measured using the Bradford Assay.

The amount of 30 μg of cytoplasmic proteins was subjected to SDS-PAGE on a 10% polyacrylamide gel and then electroblotted onto a nitrocellulose membrane. The blotted PVDF membrane was blocked in freshly prepared 5%-nonfat dry milk for 1 h at room temperature with constant agitation, then incubated with anti-SVCT2 (sc-9926), anti-SVCT1 (sc-9923) and β-tubulin primary antibodies (1: 200 dilution) (sc-9935) 2 h with agitation at room temperature. After washing by TBST three times and incubation with the donkey Anti-Goat secondary antibody (1: 2000 dilution) in 5% milk for 40 min with agitation at room temperature before visualization.

siRNA transfection

For siRNA transfection, cells were transfected with optimized concentration (7.5 pmol for fluorescence, 35 pmol for western blot) of SVCT2 siRNA and lipofectamine 2000 Reagent mixture. Oligounucleotides were diluted in Opti-MEM (Invitrogen) medium and added to the transfection reagent solution. Cells were incubated in this final mixture for 6 h at 37 ^{0}C. Afterward, DMEM with 10% fetal bovine serum and antibiotics was added to the cells and incubated for 72 h at 37 ^{0}C. Then the cells were added into our product for 30 min, washed by PBS 2 times and then stained with DAPI for 5 min.

Imaging/analysis of SVCTs expression in cells

After transfection of siRNA in HEK-293T and HepG2 cells for 72 h or adding PMA (100 nM) for 12 h, the cells were cultured in RPMI 1640 and DMEM medium containing RB-A-Vc (100 μM) for 30 min. Then the medium was removed, the cells were counterstained with DAPI after they were fixed in ice-cold 4% paraformaldehyde and analyzed by confocal fluorescence microscopy. The efficiencies of siRNA-depression and PMA-promotion of SCVTs expression was evaluated by fluorescence spectrometry (excitation at 560 nm, emission at 600 nm) using a spectral scanning multimode reader.

Results and discussion

Synthesis and characterization of RB-A-Vc

To synthesize such a fluorophore-conjugated vitamin C for SVCTs imaging, our strategy is to introduce fluorescent Rhodamine B (RB) derivatives to the C-6 hydroxy group of ascorbic acid. Two C-6 substituted esters, Rhodamine B-ascorbic acid ester (RB-Vc, **1**) and Rhodamine B-aminoheanoic acid-ascorbic acid ester (RB-A-Vc, **2**) were synthesized (Fig.1, Scheme 1). It was found that RB-AA derived by directly conjugating RB to AA is liable to hydrolysis. The hydrolysed RB dye is positively charged and can pass through the cell membrane and brings undesired fluorescence, raising the background and disturbing the observation of probe/SVCTs complexes. In an attempt to improve the stability of fluorophore-conjugated vitamin C, we chose a 6-aminohexyl chain to serve as the linker jointing AA and the fluorescent moiety (RB). We reasoned that use of this long spacer arm would keep the bulky fluorophore away from the vicinity of the binding region of AA skeleton, which benefit the stability of the ester and facilitate the probe to exhibit its binding

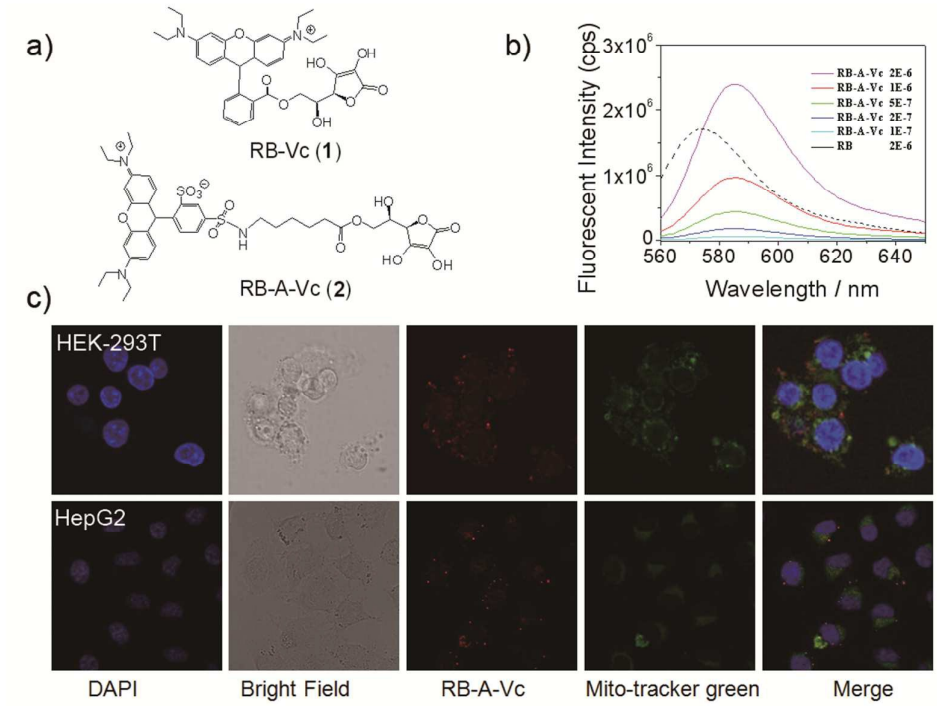

Fig.1 a) Chemical structures of RB-VC (1) and RB-A-Vc (2); b) Fluorescence spectra of RB-A-Vc probe (solid lines) and Rhodamine B (dash line); c) confocal fluorescent images of HEK-293T and HepG2 cells that were fixed with 4% paraformaldehyde and permeabilized with 0.1% Triton X-100, stained with RB-A-Vc (red), DAPI (blue) and Mito-tracker green (green). Merged images show the colocalization of mitochondria with SVCTs/RB-A-Vc complexes.

activity. Moreover, sulforhodamine B were used as fluorescent material because it is negatively charged and difficult to pass through cell membrane.[21] RB-A-Vc was synthesized in two steps.

The first step is to trigger the reaction of 6-aminoheanoic acid with L-ascorbic acid in sulfuric acid, to produce aminoheanoic acid-ascorbic acid ester (A-Vc). The second step is to conjugate sulforhodamine B onto A-Vc ester using 4-dimethylaminopyridine as a catalyst. The probe RB-A-Vc was purified and identified by liquid chromatography-mass spectrometry and characterized by fluorescent spectrometry (Fig. 2). The introduction of 6-aminohexyl spacer also brings 11 nm redshift in the emission wave-length of RB-A-Vc to RB (Fig. 1B). As we expected, RB-A-Vc shows a very good stability, in which less than 2% of original compound is hydrolysed in PBS buffer (pH 7.2) within 3 days.

Specificity of RB-A-Vc/SVCTs binding

The target and imaging mechanism is based on the specific interaction between the probe RB-A-Vc and SVCTs that expressed in cells. When AA is present, however, this process is more likely undergoing a competitive mechanism. We wondered whether exogenetic and endogenetic AA deteriorate the uptake of probe RB-A-Vc and thus have influences on SVCTs imaging. For this regard, the extracted cytoplasmic proteins of HEK-293T and HepG2 cells were subjected to native-PAGE. The RB-A-Vc (50 μM) mixed with different concentration of ascorbic acid (0 to 1 mM) in staining

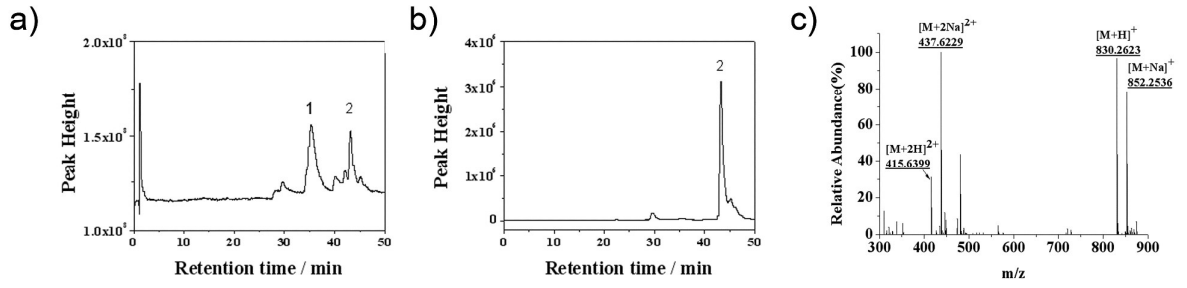

Fig. 2 UHPLC-ESI-MS/MS analysis of RB-A-Vc. (a) TIC spectra of the crude products of the reaction; **1** is assigned to sulforhodamine B chloride and **2** is assigned to the probe RB-A-Vc; (b) EIC spectra of RB-A-Vc; (c) MS spectra of RB-A-Vc extracted from TIC, in which $[M+H]^+$ of RB-A-Vc is 830.26, $[M+2H]^{2+}$ is 415.64, and $[M+2Na]^{2+}$ is 437.63. The detection of the expected molecular species indicates that the product of the reaction is successful.

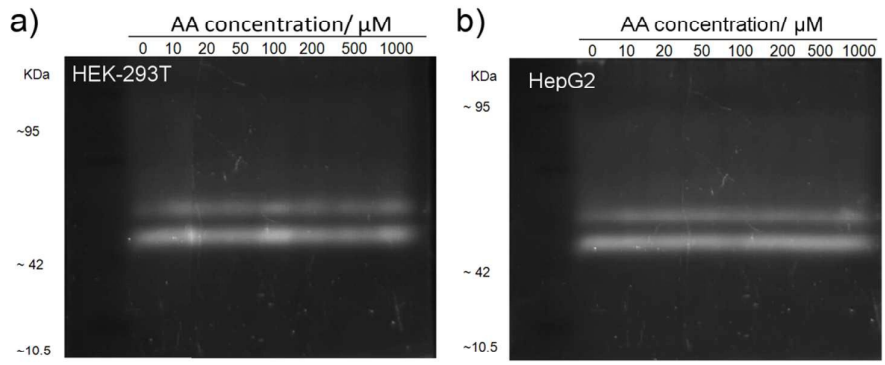

Fig.3 Native-PAGE of extracted cytoplasmic proteins of HEK-293T and HepG2 cells. SVCTs seem to preferentially bind 50 μM RB-A-Vc even in the presence of a high concentration of AA (1 mM).

buffer were employed to stain the proteins. With the increase of AA/RB-A-Vc ratio in staining buffer, in which AA brings competition with RB-A-Vc/SVCTs binding, the fluorescence of RB-A-Vc did not attenuate compared with the control (AA concentration is 0) (Fig. 3). SVCTs seem to preferentially bind 50 μM RB-A-Vc even in the presence of a high concentration of AA (1 mM). It seems that no matter low or high AA concentration, SVCTs binds with RB-A-Vc preferentially. We explain this by considering the affinity of RB-A-Vc against SVCTs is higher than that of AA. This observation is well coincident with the previous findings that C6-OH derived AA esters usually exhibit higher affinity against SVCT over the endogenous AA.[22,23] Thus, it is not necessary to be worried about the AA influences on SVCTs imaging by competition with RB-A-Vc binding. Moreover, the high affinity leads to a fast binding and slow dissociation of RB-A-Vc/SVCTs complexes, greatly facilitates the fluorescent imaging of the complexes in a relatively stable state.

Fluorescent imaging of SVCTs in the fixed cells

Prior to the living cell visualization experiments, we first examined the applicability of the synthesized RB-A-Vc for SVCTs imaging in the fixed cells. In this experiment, the fixed human HEK-293T and hepatoma HepG2 cells, which were treated with 4% paraformaldehyde and permeabilized with 0.1% Triton X-100, were employed for intracellular SVCTs monitoring. After treating the fixed cells with 100 μM RB-A-Vc, we found the red fluorescence produced by SVCT2/RB-A-Vc fast entered into the fixed cells by using the laser scanning confocal microscopy. A mitochondria tracker, Mito-tracker green, was then used to stain mitochondria in HEK-293T cells. Interestingly, it was found that the locations of SVCT2/RB-A-Vc represented by red fluorescence are highly coincident to that of mitochondria (green fluorescence). This implies that SVCT2 would be primarily located in mitochondria, which is consistent with the previous studies.[24,25] Nearly no fluorescent signals could be seen on the membrane of HEK-293T cell, implying the level of SVCTs in cell membrane is very low. Confocal colocalization experiments with anti-SVCT2 revealed that most of the SVCT2 immunoreactivity was associated with mitochondria, and very low immunoreactivity at the plasma membrane (Fig. 4). This confirmed our findings obtained by using RB-A-Vc imaging.

Fluorescent imaging of SVCTs in the living cells

To gain further insight into fluorescent sensing and imaging of SVCTs in living cells, we applied RB-A-Vc for directly staining SVCTs in living HEK-293T and HepG2 cells. A fundamental of SVCTs function is their potent activation by sodium ions. Uptake of AA by living cells required the presence of Na^+ ions, with the cooperation of Ca^{2+} and Mg^{2+} ions.[26] Therefore, in all tests, the probe RB-A-Vc was dissolved in 10 mM HEPES containing 135 mM NaCl, 5 mM KCl, 2.0 mM $CaCl_2$ and 1.0 mM $MgCl_2$. The fluorescence confocal microscopy analysis provided that RB-A-Vc could fast enter into the living cells within 30 min. The RB-A-Vc stained living cells were then fixed with paraformaldehyde and permeabilized with Triton X-100, followed by staining steps with DAPI (nuclei, blue) and Mito-tracker green (mitochondria, green). Confocal fluorescent images reveal the successful binding between RB-A-Vc and intracellular SVCT2, showing SVCT2 is mainly localized near to the positions of mitochondria (Fig. 5a). We also addressed this issue by performing colocalization experiments using RB-A-Vc in combination with antibodies against protein markers, in which anti-SVCT2, anti-SVCT1, anti-COXIV for mitochondria, anti-GLUT1 for plasma membrane (in the case of HepG2 cells) were employed for subcellular staining. It must to note that immunofluorescence antibodies including anti-SVCT2 and anti-SVCT1 bind SVCTs in a quite different manner from AA or RB-A-Vc, thereby not interfering the forming of SVCTs/RB-A-Vc complexes.[27] Confocal colocalization experiments with anti-SVCT2 and anti-organelle protein markers revealed that most of the SVCT2 immunoreactivity was associated with mitochondria, with minor colocalization at the endoplasmic reticulum and very low immunoreactivity at the plasma membrane. The transporter SVCT1 is absent from HEK-293T

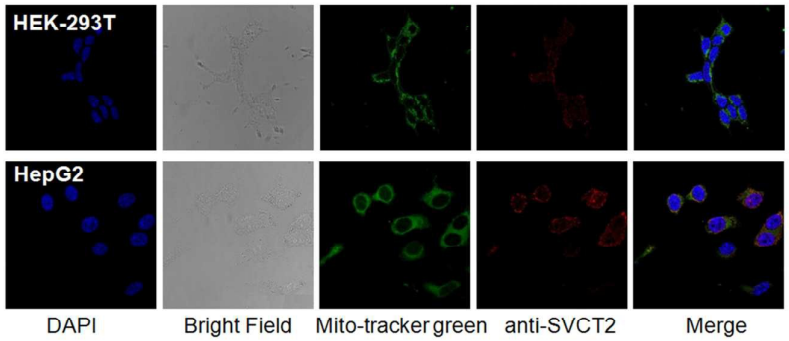

Fig.4 Confocal colocalization of anti-SVCT2 (in red) with mitochondria dye mito-tracker green (in green) in HEK-293T (the upper) and HepG2 cells (the bottom). Cells were fixed with 4% paraformaldehyde and permeabilized with 0.1% Triton X-100, incubated with the primary anti-SVCT2 and then the second antibody Cy3-conjugated affiniPure Donkey Anti-Goat IgG (H+L) (red), stained nuclei with DAPI (blue).

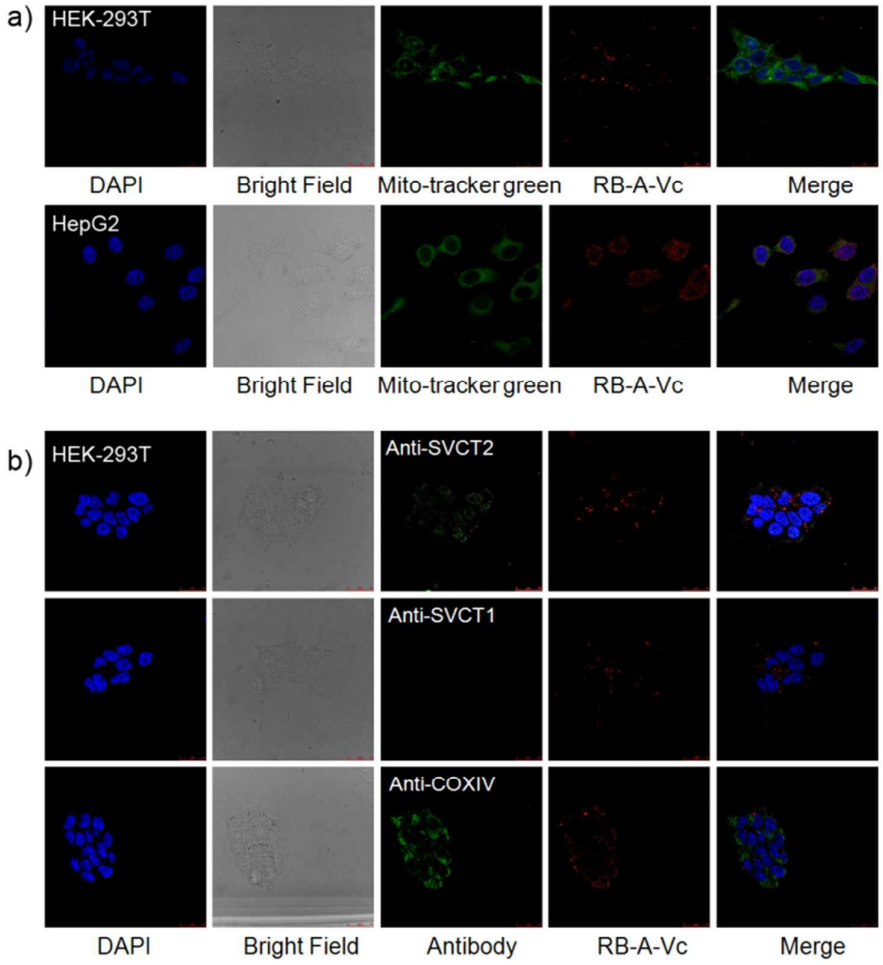

Fig.5 a) Confocal colocalization of SVCT2/RB-A-Vc with Mito-tracker green in living HEK-293T (the upper) and HepG2 (the bottom) cells; b) confocal colocalization of RB-A-Vc with anti-SVCT2, anti-SVCT1 and anti-COXIV in HEK-293T cells.

cells. Unlike HEK-293T cells, both SVCT1 and SVCT2 were detected in HepG2 cells. SVCT2 was primarily found at the positions of mitochondria, slightly observed on the membrane. Meanwhile, a large amount of SVCT1 was observed on the membrane of HepG2 cells. The intracellular distributions of SVCTs depicted by antibodies were in accordance with that monitored by RB-A-Vc probe. RB-A-Vc could be used as a living cell fluorescence probe to realize the subcellular localization.

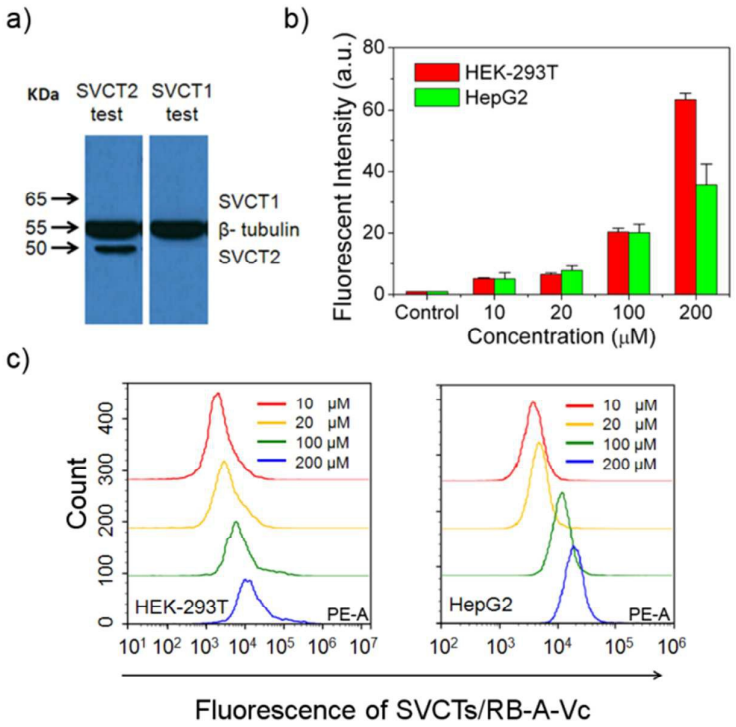

Fig.6 a) western blot of SVCT2 and SVCT1 expression in HEK-293T cells, b) the dosage effect of RB-A-Vc concentration on fluorescence responses by confocal fluorescent imaging ; c) the dosage effect measured by flow cytometry analysis.

It is note that the isoelectric point (pI) of the synthesized RB-A-Vc was measured as 5.2. Under the physiological pH conditions (pH 7.2), RB-A-Vc became negatively-charged and difficult to pass through the cell membrane without the aid of transporters.[28] To further confirm RB-A-Vc was transported by SVCTs, we examined the specificity of RB-A-Vc against SVCTs by Western blot assay. Result indicates there is only SVCT2 was identified at ~50 KDa, but no SVCT1 (at 65 KDa) was found in HEK-293T cells (Fig. 6).

Dosage effect of RB-A-Vc on SVCTs imaging

To investigate the dosage effect of RB-A-Vc on SVCTs imaging, different concentration of RB-A-Vc was employed to the cultured living cells. Fluorescence measurement by microplate reader revealed that, in a wide range of RB-A-Vc concentration (form 10 to 200 μM), the fluorescence responses were continuously increased both for HEK-293T and HepG2 cells (Fig. 6b). This phenomenon was also observed by confocal fluorescent imaging and flow cytometry analysis (Fig. 6c). From 10 to 200 μM of RB-A-Vc, the fluorescence responses of RB-A-Vc/SVCTs complexes in HEK-293T cells became brighter, which were predominately located in cellular plasma near the mitochondria. When RB-A-Vc concentration is higher than 200 μM, however, redundant fluorescent signals were observed on the cell membrane and in the adjacent areas between the individual cells. Considering the fact that HRK-293T cells does not express high level SVCTs on the membrane, the emerging fluorescence are more likely generated from the non-selective interactions between the probe and biomolecules on cell surface. To avoid the non-selective interactions, 100 μM of RB-A-Vc was selected for intracellular SVCTs investigation.

Indication of changes in SVCTs expression in living cells

After the validation of RB-A-Vc's function in SVCTs labelling and localization, we asked whether it could indicate the changes of SVCTs expression in living cells. For this purpose, we first examined the situation of suppression of SVCTs expression. Human HEK-293T cells were transfected with SVCT2 siRNA or negative control (NC) siRNA within 72 h, and then SVCT2 content was examined by western blot. To the siRNA treated 293T cells, 100 μM of RB-A-Vc was added and then visualized by confocal fluorescent imaging. HEK-293T cells showed decreased fluorescence intensity after SVCT2 siRNA treatment (Fig. 7a). Fluorescence analysis and Western blotting revealed a decreased SVCT2 expression by approximately 60% (Fig. 7b, c). FACS analysis (flow cytometry) also substantiated the decrease of fluorescence of RB-A-Vc after transfection of SVCT2 siRNA. This implies RB-A-Vc can indicate the down-regulation of SVCT2 expression in living cells.

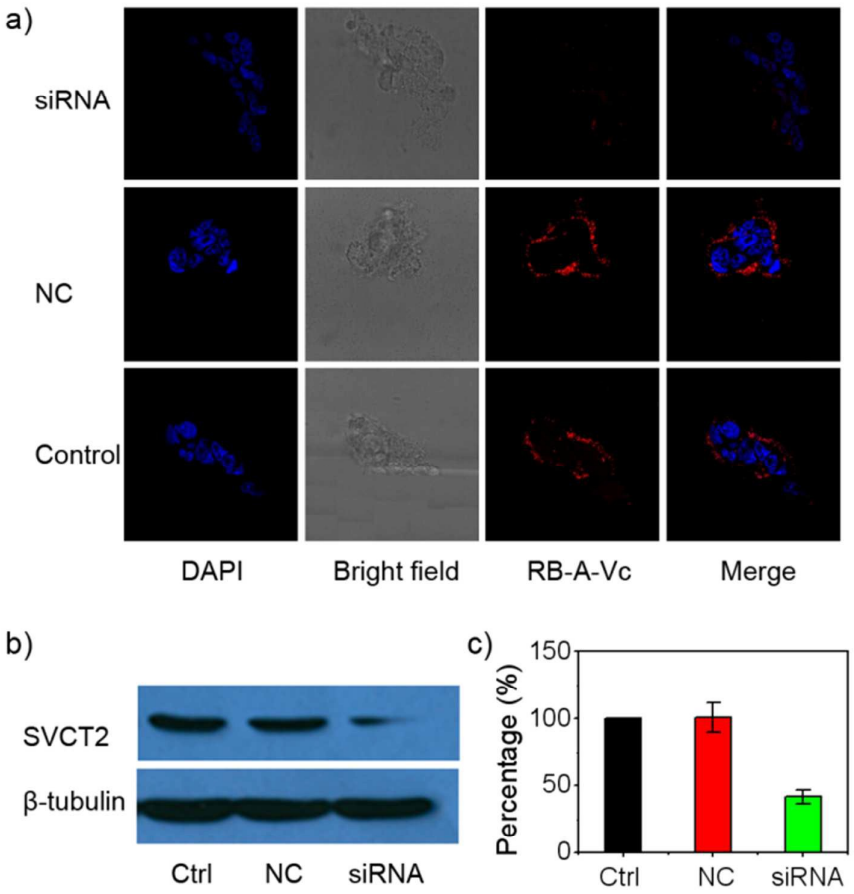

Fig.7 Use of SVCT2 siRNA for silencing SVCT2 expression produced a major decreases in mitochondrial. a) immunoblotting revealed decreased SVCT2 protein expression by approximately 75%; b) western blot and c) fluorescence analysis of SVCT2 expression in SVCT2 siRNA treated HEK-293T cells.

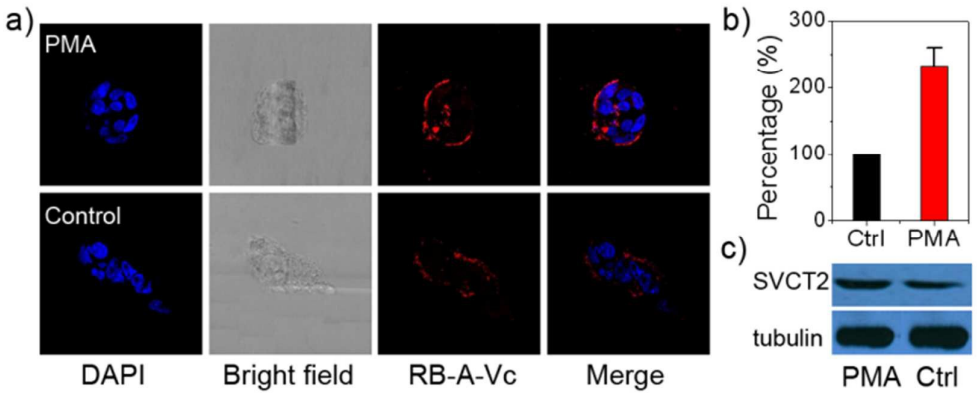

Fig.8 PMA induces an up-regulated SVCT2 expression in HEK-293T cells. a) RB-A-Vc visualizes the PMA-induced up-regulation of SVCT2 expression; b) fluorescence analysis and c) western blot of SVCT2 expression in PMA treated HEK-293T cells

We then validated the function of RB-A-Vc probe by indicating the promotion of SVCTs expression in living cells. Phorbol 12-myristate 13-acetate (PMA) is a nonselective protein kinase-C activator, and it was reported to cause a large increase in SVCT2 expression.[22,29,30] In this experiment, we added 100 nM PMA to HEK-293T cells to induce an up-regulated SVCTs expression, and then extracted the cytoplasmic proteins to conduct Western blot experiment.

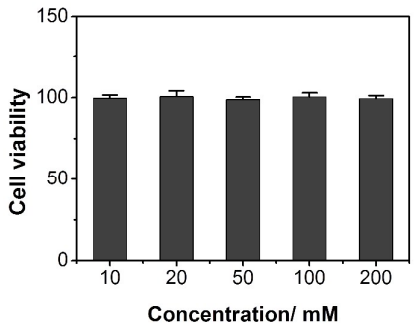

Fig.9 No observable cytotoxicity of RB-A-Vc (10-200 mM) to the HEK-293T cells (MTS assay).

After exposure with PMA, the expression of SVCT2 greatly increased. Compared with the control, the intensity of fluorescence of RB-A-Vc increased obviously after adding 100 nM PMA. Fluorescence analysis and Western blotting revealed up-regulated SVCT2 protein expression by approximately 220% (Fig. 8). This result suggests that RB-A-Vc could indicate not only the down-regulation but also the up-regulation of SVCT2 expression. Together, these results support the notion that RB-A-Vc is a potent fluorescent probe to indicate changes of SVCTs which are responsible for the transportation of ascorbic acid into cells.

Cytotoxicity of probe RB-A-Vc

Moreover, the cytotoxicity of probe RB-A-Vc to HepG2 cells was measured by using a water soluble tetrazolium salts (3-(4,5-dimethylthiazol-2-yl)-5-(3-carboxymethoxyphenyl)-2-(4-sulfophenyl) -2H-tetrazolium) (MTS) assay. As shown in Fig. S6 (ESI†), the cellular viability in the presence of either RB-A-Vc or sulforhodamin B chlorine was estimated to be greater than 98% after 24 h with increasing concentration of dyes. Hence, RB-A-Vc could be regarded to be low in cytotoxicity and suitable for living cell imaging.

Conclusions

In summary, we have presented the synthesis and application of RB-A-Vc, a new small molecule fluorescent probe for selective fluorescence imaging of SVCTs in living cells. This probe features visible excitation and emission profiles, ease of entering into cells, high selectivity for SVCTs, and can monitor up-regulation or down-regulation of SVCTs expression in living cells. We emphasize this small-molecule probe is suitable for subcellular localization of SVCTs in living cells. This study provides a potent tool for simultaneously monitoring the level and distribution of intracellular SVCTs, which is probably more meaningful to evaluate the changes induced by exoteric stimulations. We propose that this probe for SVCTs imaging and the corresponding method can be extended to the imaging of other cell lines, tissues, and species.

Acknowledgements

The work was financially supported by grants from the National Basic Research Program of China (No. 2014CB932003), the Strategic Priority Research Program of the CAS (No. XDB14030300), the National Natural Science Foundation of China (Nos. 21375142 and 21300076), and the special fund for public benefit from Ministry of Environmental Protection of China (No. 201309045).

Notes and references

1 F.E. Harrison and J.M. May, *Free Radic. Biol. Med.*, 2009, **45**, 719.
2 I. Savini, A. Rossi, C. Pierro, L. Avigliano and M.V. Catani., *Amino Acids*, 2008, 34, 347.
3 M. Hediger, *Nat. Med.*, 2002, **8**, 445; 1(d) I. Savini, M.V. Catani, R. Arnone, A. Rossi, G. Frega, D.D. Principe, L. Avigliano, *Free Radic. Biol. Med.*, 2007, **42**, 608.
4 J.M. May, *Br. J. Pharmacol.*, 2011, **164**, 1793.
5 J.M. May, Z.C. Qu and S. Mendiratta, *Arch. Biochem. Biophys*., 1998, **349**, 281.
6 S.B. Nimse and D. Pal, *RSC Adv.*, 2015, **5**, 27986.
7 H. Tsukaguchi, T. Tokui, B. Mackenzie, U. Berger, X. Chen, Y. Wang, R. Brubaker and M. Hediger, *Nature*, 1999, **399**, 70.
8 F. Nualart, L. Mack, A. García, P. Cisternas, E.R. Bongarzone, M. Heitzer, N. Jara, F. Martínez, L. Ferrada, F. Espinoza, V. Baeza, K. Salazar, *J. Stem Cell Res. Ther.*, 2014, **4**, 209.
9 J.C. Reidling and S.A. Rubin, *J. Nutr. Biochem.*, 2011, **22**, 344; 3(d) F.E. Harrison and J.M. May, *Free Radic. Biol. Med.*, 2009, **46**, 719.
10 F.E. Harrison, S.M. Dawes, M.E. Meredith, V.R. Babaev, L. Li and J.M. May, *Free Radic. Biol. Med.*, 2010, **49**, 821.
11 S. Sotiriou, S. Gispert, J. Cheng, Y.H. Wang, A. Chen, S. Hoogstraten-Miller, G.F. Miller, O. Kwon, M. Levine, S.H. Guttentag and R.L. Nussbaum, *Nat. Med.*, 2002, **8**, 514.
12 A.I. Acuña, M. Esparza, C. Kramm, F.A. Beltrán, A.V. Parra, C. Cepeda, C.A. Toro, R.L. Vidal, C. Hetz, I.I. Concha, S. Brauchi, M.S. Levine and M.A. Castro, *Nat. Commun.*, 2013, **4**, 2917.
13 H.R. Harris, N. Orsini and A. Wolk, *Eur. J. Cancer*, 2014, **50**, 1223.
14 V. Khurana, D. Kwatra, D. Pal, A.K. Mitra, *Int. J. Pharm.*, 2014, **474,** 14.
15 X. Xu, E. Yu, L. Liu, W. Zhang, X. Wei, X. Gao, N. Song and C. Fu, *Eur. J. Cancer Prev.*, 2013, **22**, 529.
16 S. Huang, F. Zhu, Q. Xiao, W. Su, J. Sheng, C. Huang and B.Hu, *RSC Adv.*, 2014, **4**, 46751.
17 J. Kim, T. Kino, H. Kato, F. Yamamoto, K. Sano, T. Mukai and M. Maeda, *Chem. Pharm. Bull.*, 2012, **60**, 235.
18 G.H. Mun, M.J. Kim, J.H. Lee, H.J. Kim, Y.H. Chung, Y.B. Chung, J.S. Kang, Y.I. Hwang, S.H. Oh, J.G. Kim, D.H. Hwang, D.H. Shin and W.J. Lee. *J. Neurosci. Res.*, 2006, **83,** 919.
19 M.E. Meredith, F.E. Harrison, J.M. May, *Biochem. Biophys. Res. Commun.*, 2011, **414**, 737.
20 L. Mardones, F.A. Zúñiga, M. Villagrán, K. Sotomayor, P. Mendoza, D. Escobar, M. González, V. Ormazabal, M. Maldonado, G. Oñate, C. Angulo, I.I. Concha, A.M. Reyes, J.G. Cárcamo, V. Barra, J.C. Vera and C.I. Rivas. *Free Radic. Biol. Med.*, 2012, **52**, 1874.
21 O. Boussif, F. Lezoualc'h, M.A. Zanta, M.D. Mergny, D. Scherman, B. Demeneix and J.P. Behr, *Proc. Natl. Acad. Sci. USA*, 1995, **92**, 7297.

22 S. Manfredini, B. Pavan, S. Vertuani, M. Scaglianti, D. Compagnone, C. Biondi, A. Scatturin, S. Tanganelli, L. Ferraro, P. Prasad, A. Dalpiaz, *J. Med. Chem.*, 2002, **45**, 559.
23 A. Dalpiaz, B. Pavan, M. Scaglianti, F. Vitali, F. Bortolotti, C. Biondi, A. Scatturin, S. Tanganelli, L. Ferraro, P. Prasad, S. Manfredini, *J. Pharm. Sci.*, 2004, **93**, 78.
24 C. Muñoz-Montesino, F.J. Roa, E. Peña, M. González, K. Sotomayor, E. Inostroza, C.A. Muñoz, I. González, M. Maldonado, C. Soliz, A.M. Reyes, J.C. Vera and C.I. Rivas, *Free Radic. Biol. Med.*, 2014, **70**, 241.
25 M. Burzle and M.A. Hediger. *Curr. Top. Membr.*, 2012, **70**, 357.
26 Godoy, V. Ormazabal, G. Moraga-Cid, F.A. Zúñiga, P. Sotomayor, V. Barra, O. Vasquez, V. Montecinos, L. Mardones, C. Guzmán, M. Villagrán, L.G. Aguayo, S.A. Oñate, A.M. Reyes, J.G. Cárcamo, C.I. Rivas and J.C. Vera, *J. Biol. Chem.*, 2007, **282**, 615.
27 Varma, K. Sobey, C.E. Campbell and S.M. Kuo, *Biochemistry*, 2009, **48**, 2969.
28 Luo, Z. Wang, V. Kansara, D. Pal and A. Mitra, *Int. J. Pharm.*, 2008, **358**, 168.
29 H. Qiao and J.M. May, *Free Radic. Biol. Med.*,2009, **46**, 1221.
30 V. Ulloa, M. García-Robles, F. Martínez, K. Salazar, K. Reinicke, F. Pérez, D.F. Godoy, A.S. Godoy and F. Nualart, *J. Neurochem.*, 2013, **127**, 403.

A fluorophore-conjugated ascorbic acid functions for visualization of sodium vitamin C transporters in living cells

Junfa Yin, Yuanyuan Song, Ning Zhang, Tian Xu and Hailin Wang

DOI:

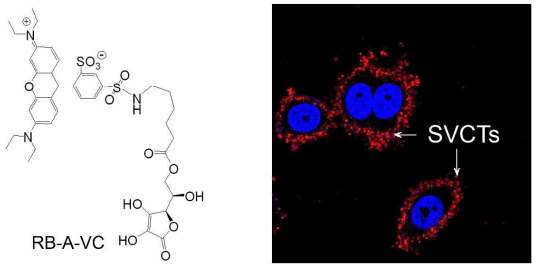

We designed and synthesized a fluorophore-conjugated ascorbic acid, and found that this compound is capable of selectively visualizing the level and changes of intracellular SVCTs in living cells.